https://doi.org/10.48048/tis.2024.7677

Studies on Nano-Indentation and Corrosion Behavior of Diamond-Like Carbon Coated Stainless Steel (316L)

Suresh Kolanji[1,*], Manikandan Sivakatatcham[1] and Sivaprakasam Palani[2]

[1]Department of Mechanical Engineering, FEAT, Annamalai University, Tamil Nadu, India
[2]Department of Mechanical Engineering, College of Engineering, Center of Excellence Nano Technology, Addis Ababa Science and Technology University, Addis Ababa, Ethiopia

([*]Corresponding author's e-mail: sureshsathy21@gmail.com)

Received: 2 November 2023, Revised: 1 December 2023, Accepted: 22 December 2023, Published: 20 March 2024

Abstract

Stainless steel 316L is commonly used in biomedical applications like dental implants, surgical tools, and other devices due to its corrosion resistance and cost-effective materials compared to other biomaterials. It must be enhanced since 316L SS has a relatively low hardness and wear resistance. The coating process includes applying functional materials to the surface to modify and give it the desired properties. This study used a PVD technique for coating diamond-like carbon (DLC) on the surface of 316L stainless steel to enhance its material surface properties. The coated and uncoated SS316 surfaces were exposed to nanoindentation (ultra-nano hardness tester (UNHT3) and electrochemical corrosion tests such as open circuit potential, potentiodynamic polarization, and electrochemical impedance spectroscopy in simulated body fluids at 37 °C. SEM characterized the morphologies and compositions of the surfaces with energy-dispersive X-ray spectroscopy.

Keywords: Stainless steel 316L, DLC coating, Nano-indentation, Electrochemical corrosion, SBF

Introduction

Stainless steel 316L is one of the most extensively used materials in marine industries, nuclear reactors, and biomedical implants due to its corrosion resistance, low cost, increased mechanical properties, and good biocompatibility [1]. Particularly for medical applications, such as medical equipment, dental and orthopedic implants, spinal rods, skull plates, stents, and other devices, because of its favorable combination of mechanical and corrosion properties and affordability compared to other metallic materials used for implants [2]. Various factors such as chemical composition, microstructure, processing methods, and surface treatment can influence the properties of biomaterial SS 316L. These factors can affect the mechanical properties, corrosion resistance, and biocompatibility of the material and thus should be carefully considered in the selection and design of such implants [3]. The components are made for implants, especially hip replacement materials such as stainless steel, cobalt chrome, Ti, and Ti alloys [4]. The functional grade materials' performance, such as hardness, wear resistance, and electrical and optical properties, has been enhanced by incorporating nanomaterials [5-10]. The PVD process investigated the wear properties of SS316 LVM using AlTiN coating. The relationship between various factors' influences on wear rate and COF were investigated. The coating has been found to have enhanced the wear behavior of SS316LVM [11].

DLC (Diamond-Like Carbon) films possess numerous desirable properties that make them appropriate for biomedical applications. These characteristics encompass high levels of hardness, low friction coefficient, strong resistance to corrosion, and good biocompatibility [12]. Surface modification of stainless steel by applying DLC (Diamond-Like Carbon) films is crucial for enhancing its wear resistance and self-lubricating properties. The low friction coefficient of DLC films makes ideal uses in sliding or rolling contact situations. Furthermore, DLC films can improve stainless steel's corrosion resistance and biocompatibility, which is especially valuable for medical implants and devices. Electrochemical corrosion tests were conducted to evaluate the corrosion resistance of DLC films on 316L stainless steel, and the results showed that the DLC film demonstrated superior resistance to pit corrosion when compared to the 316L substrate in 3.5 % NaCl solution [13].

DLC coating can be a viable and effective solution for protecting stainless steel against corrosion in environments with varying water concentrations [14]. DLC coating on aluminium 5051 has enhanced its mechanical and tribological properties, thereby developing more durable and efficient materials [15].

Kumari *et al.*, successfully created uniform and homogenous thin coatings (DLC) on a stainless steel surface without needing a thin interlayer. The omission of an interfacial layer streamlines the coating process and reduces costs associated with DLC coating on stainless steel. Moreover, the study highlights the DLC coating's ability to adhere well to stainless steel without requiring an interfacial layer [16].

The study of biomaterial corrosion is critical for improving the performance and safety of medical implants and devices. It is now possible to improve medical results and overall quality of life by understanding more about the corrosion behaviour of biomaterials [14]. The corrosion resistance and micromechanical characteristics of the fusion-fabricated 316L stainless steel parts of the laser powder bed. It indicates the most favourable micromechanical properties, the smallest grain size and the lowest areal surface roughness [17]. No established principles existed for discovering bone-bonding materials until the authors suggested in 1991 that assessing apatite formation on a material's surface in a cellular simulated body fluid (SBF) could determine its bone-bonding capacity without animal experiments. Numerous novel bone-bonding bioactive materials with diverse functions based on metals (Ti) and their alloys have been created using SBFs [18].

The corrosion characteristics of SS316L are 2 distinct simulated body fluids, namely Fusayama Meyer (pH = 4.8) and Hank solution (pH = 7.36). The study deduced that the pH level of simulated body fluids is a critical factor that influences the corrosion characteristics of SS316L [19]. The coating acts as a proficient barrier layer that shields against corrosive ions, thereby impeding corrosion and prolonging the lifespan of the implant [20]. The research demonstrated the significance of the passive film created on the surface of SS316L in preventing it from corrosion in SBFs [21].

Tassin *et al.* [22] attempted to use the laser surface alloying process to increase the wear resistance of stainless steel 316L. The researchers used chromium and titanium carbides for alloying, and significant improvement was made without any adverse effects. Li *et al.* [23] applied a wear-resistant layer on stainless steel 316L, demonstrating adequate protection against adhesion, abrasion, and oxidation mechanisms compared to untreated material. A novel strategy for enhancing the wear resistance of stainless steel 316L was developed by Dearnley and Aldrich-Smith [24], and it involves using thin hard coatings. If the surfaces are adequately prepared, each of the options the writers offered successful outcomes. Alvi *et al.* discussed high-temperature wear behavior to increase the stainless steel 316L's wear resistance [25].

Stainless steel 316L has been widely used in biomedical applications for internal support and tissue substitutes over many years. Its suitable strength, fair corrosion resistance, and cost-effectiveness have made it a popular choice for replacement joints, dental roots, and general muscle and joint repair. Additionally, their use periods are significantly limited because of their poorer resistance to abrasion and wear, which is followed by a formation of wear particles at the defect site, a deficiency of osseointegration, and most importantly, the body's release of incompatible metal ions like Ni, Cr, and Mo [26]. Surface modification of alloy implants via physical vapor deposition (PVD) is an efficient method of improving functionality [27]. Enhancing hardness, wear, corrosion resistance, and biocompatibility are the primary uses of PVD in the biomedical field [28]. PVD coatings can be tailored to provide a combination of improved hardness, corrosion resistance, and other desirable properties, making them a versatile solution for enhancing the performance of stainless steel and extending its range of applications. The application of nanocomposite coats has the potential to concurrently enhance the bioactivity, resistance to corrosion, and osseointegration of metallic substrates, resulting in the formation of chemical and physical bonds with host tissues [26].

There are several limitations and gaps in the research on biomaterial SS316L. The possible medical uses of the proposed 316L surface modification technique have yet to be fully explored. Hence, current research evaluates the surface coating of diamond-like carbon (DLC) using PVD and investigate the mechanical properties such as hardness and elastic modulus using nanoindentation corrosion behavior of diamond-like carbon (DLC) coated stainless steel 316L.

Materials and methods

Material preparation

The stainless steel 316L has been purchased from Fast Well Engineering Private Limited in Mumbai. Its chemical elements, such as Chromium (Cr) at 17.5 %, Nickel (Ni) at 13.6 %, Manganese (Mn) at 1.39 %, Molybdenum (Mo) at 2.27 %, Carbon (C) at 0.03 %, Phosphorous (P) at 0.045, Sulphur (S) at 0.030 %, Silicon (Si) at 1.0 %, and Iron (Fe) for balance. The test samples were machined with 6 mm diameter and 12 mm length for experimental work.

Coating process

The sample was cut into pieces 12 mm long and 6 mm in diameter in a wire-cut discharge machine. Then, the samples are polished, and samples are washed in acetone. The diamond-like carbon (DLC) was deposited, without any interfacial layers [18] at a thickness of 3µm (approx.) through the physical vapor deposition (PVD) coating technique at Oerlikon Blazers Coating India Pvt. Ltd. Scalable Pulsed Power Plasma techniques were used for DLC coating that successfully combines the benefits of sputtering and arc evaporation under process temperature ≤ 250 °.

Nanoindentation

An ultra-nano indentation tester (Anton Paar India Limited, Haryana) with a Vickers tip indenter was used at 6 different locations on the sample. Acquisition rate at 10 Hz, approach distance and speed at 2,000 nm, maximum load at 200 mN, pause time at 3 s, and finally, loading and unloading rate at 2,400 mN/min. During the indentation test, in-built software was used to collect the data. From the data, the hardness and elastic modulus of the valves are generated. The Oliver and Pharr approach was used in the current investigation. **Figure 1(a)** shows the photographic view of the experimental setup, indicating the workpiece and the locations of indentations. **Figure 1(b)** shows the test samples for coated and uncoated samples.

Hardness (H) and Elastic modulus (E) is calculated using Eqs. (1) and (2);

$$H = \frac{Pmax\ [Maximum\ perpedicular\ load]}{Ap\ [Projected\ contact\ area]} \quad (1)$$

$$E = \frac{1-v_s^2}{\frac{1}{E_r} - \frac{1-v_i^2}{E_i}} \quad (2)$$

where, E_i=*Elastic modulus of the tip,* E_r =*Reduced elastic modulus of the indentation contact,* $v_i = Paissons\ ratio\ of\ tip$; $v_s = Paissons\ ratio\ of\ Sample$

Electrochemical test

The electrochemical tests were carried out using a three-electrode workstation at 37 °C to study the corrosion behavior of SS316L in SBF (pH 7.25) [20]. All electrochemical experiments were performed in Metrohm µ-Autolab 3 with an electrode setup (Thiyagaraja Engineering College, Madurai). To assess the corrosion behavior of SS316L, both coated (DLC) and uncoated samples were subjected to electrochemical tests using open circuit potentials, electrochemical impedance spectroscopy, and potentiodynamic polarisation techniques. In this setup (Metrohm µ-Autolab 3), Platinum acted as a counter electrode, SS 316L acted as a working electrode, and calomel acted as a reference electrode. **Table 1** shows the iron concentrations of SBFs.

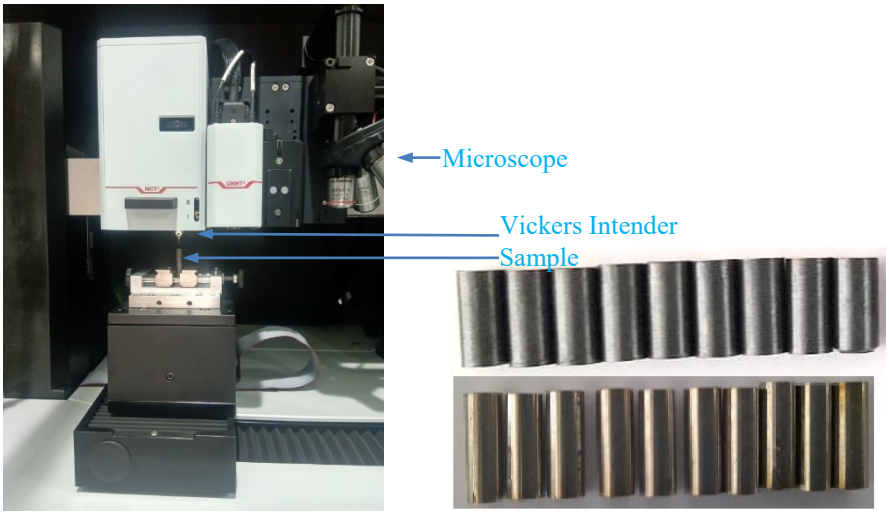

(a) (b)

Figure 1 (a) Ultra-nano indentation tester and (b) Test samples.

Figures 2 and **3** show the photographic view of the electrochemical test setup and protocol for analysis of the corrosion behavior of the samples. The samples were placed in the solution for 30 min to obtain a steady state of OCP, i.e., Ecor and Icor values. Then, EIS and PP experiments were conducted. Using an equivalent electric circuit, the EC-Lab-V10.40 software (Zfit) validated the experimental data in the electrochemical impedance spectroscopy test.

Table 1 Iron concentrations of SBF.

Concentrations	Na^+	K^+	Mg^{2+}	Ca^{2+}	Cl^-	HCO_3^-	HPO_4^{2-}	SO_4^{2-}	pH
Amount of iron in 1Lt	142.0	5.0	1.5	2.5	147.8	4.2	1.0	0.5	7.250

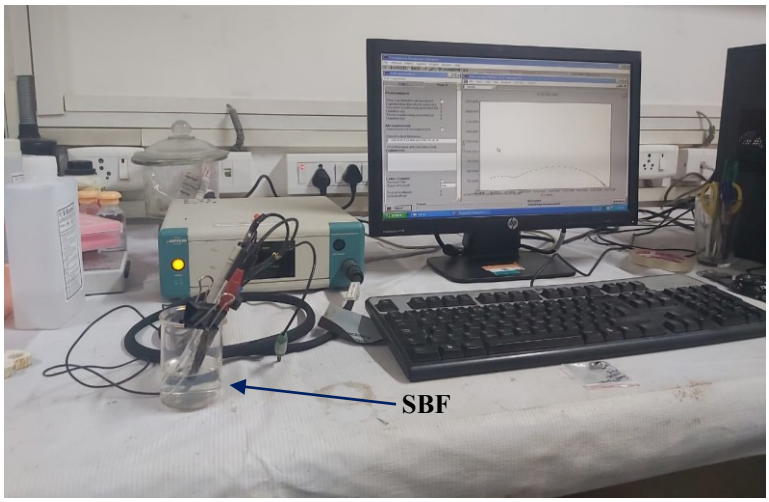

Figure 2 Electrochemical test setup.

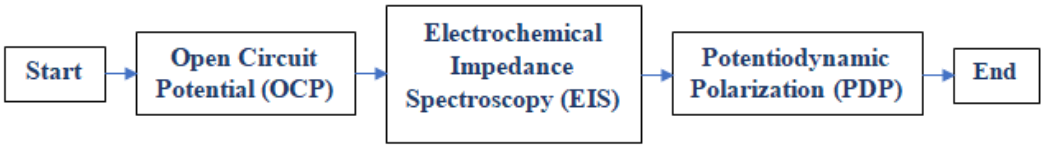

Figure 3 Electrochemical test protocol.

Surface characterization techniques

Diamond-like carbon-coated, and uncoated SS316L surfaces have been characterised via SEM and EDS. A Jeol-Jsm-It200 model instrument (CISL, Annamalai University) was used to evaluate the surface morphologies and the elements presented on the coated and uncoated SS316L surfaces by electron dispersive X-ray spectrometry.

Results and discussion

Analysis of nanoindentation test

The primary problem associated with S316 materials is that they corrode and wear out if exposed to the physiological environment of the body for an extended period. Pitting corrosion is especially prone to affect stainless steels made of 316L [29]. The coatings offer a unique approach for reducing wear sensitivity and corrosion of 316L implant materials [30, 31].

The excellent tribological achievement, high hardness, corrosion resistance, and thermal and chemical stability of diamond-like carbon (DLC) coatings have made them an alternative option for many industries in recent years [32]. The physical and structural behaviors of the DLC coatings are contingent upon the deposition technique and adding extra elements like silicon, hydrogen, and nitrogen. These extra components influence the residual stress, the tribological features, and the hardness of the resulting film

[33]. Tissue can support a strong interface and adhere well to C implants. Furthermore, a protein layer that forms in the presence of blood halts blood clots from forming at the C surface.

W.C. Oliver *et al.* describe using load and displacement sensing indentation experiments to determine hardness and elastic modulus. The study results show that moduli can be measured to within 5 % with good technique. Additionally, they suggest exploring the analysis procedure to determine the hardness and elastic modulus of other materials beyond the 6nine materials tested in the study. Therefore, the analysis procedure has the potential to be applied to a broader range of materials for hardness and elastic modulus determination [34].

Nanoindentation is one of the advanced techniques used to find the mechanical properties of coating and thin films. The mechanical properties like hardness and modulus are calculated based on the method proposed by Oliver-Pharr. The nanoindentation has 3 stages: Loading, dwell, and unloading. The indentation depth is a crucial factor for indentation because a higher indentation depth also influences the mechanical properties of the base metal. The substrate demonstrates increased plastic deformation compared to DLC films on the SS316L substrate, indicating its superior plasticity. In **Figure 4**, the load-displacement curve illustrates the behavior of coated SS316L.

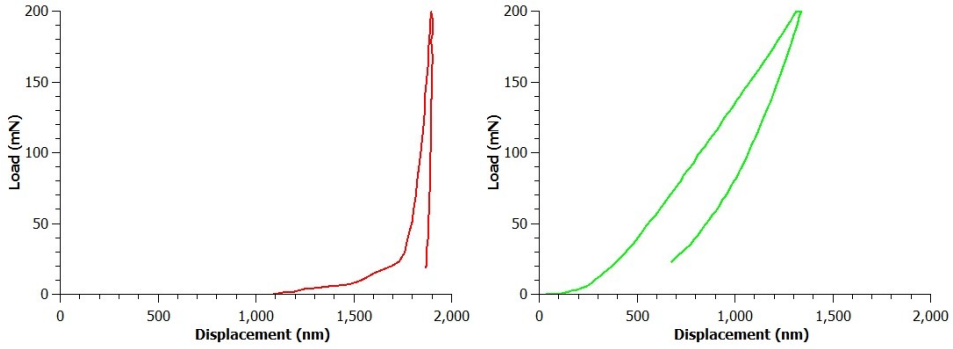

Figure 4 (a) Nanoindentation curve –Uncoated SS316L and (b) Nanoindentation curve –DLC Coated SS 316L.

From the data collected from the indentation curve, the average values for hardness and elastic modulus of the DLC films were 15.3 and 162.2 GPa, respectively. The hardness and elastic modulus values for uncoated samples were 354.33 MPa and 33.44 GPa, respectively. **Figures 4(a) - 4(b)** show that the displacement values are higher in uncoated samples than in coated samples. The hardness and elastic modulus of coated samples are better than those of uncoated samples [35]. A similar observation has been found in DLC coating of steel 15.874, 152.81 GPa respectively [36]. DLC Coating had an indentation depth of 536 nm, plastic hardness, and Young's modulus of 18 ± 0.7 and 146 ± 10 GPa, respectively [32]. The hardness values obtained from the coated surface are more than 40 times higher than uncoated samples.

Analysis of electrochemical test

Electrochemical impedance spectroscopy

Open circuit potentials (OCP) are a straightforward technique for investigating materials' corrosion characteristics (stability). It permits the examination of film formation on a test sample submerged in SBFs, with a film's potential versus time plotted; it is shown in **Figure 5**. A steady potential during EIS suggests that the film on the test sample is stable and that no significant changes in the electrochemical reactions occur at the electrode surface. An upward shift in potential reveals the development of a protective layer, whereas a steady potential shows the continuous presence of a protective layer [34]. Conversely, a decrease in potential signifies film dissolution, absence of film formation, or a break in the film's integrity. An impedance obtained in the electrochemical test (EIS) can be expressed as a complex number with a genuine part (Z'/ohm) and an imaginary part (Z"/ohm). When plotting EIS data, the Z'/ohm plot is on the X axis, and the Z"/ohm plot is on the Y axis. In the Nyquist plots, each point corresponds to an impedance value at a specific frequency, with the imaginary part being negative. The position of the impedance points on the plot indicates the frequency dependence of the impedance. Points on the right

side of the plot represent low-frequency impedance, while points on the left correspond to higher frequencies.

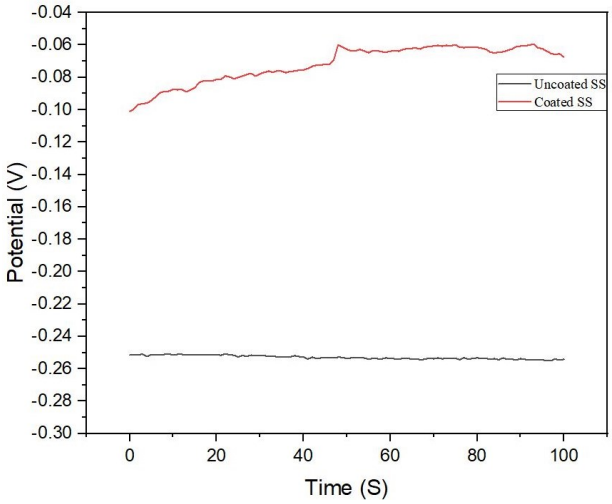

Figure 5 Potential vs Time – OCP Plot.

Furthermore, on the Nyquist plot, the impedance can be visualized as a vector or arrow with a length equal to the magnitude of the impedance (|Z|). This vector representation provides a convenient way to understand the magnitude and phase relationship of the impedance at different frequencies.

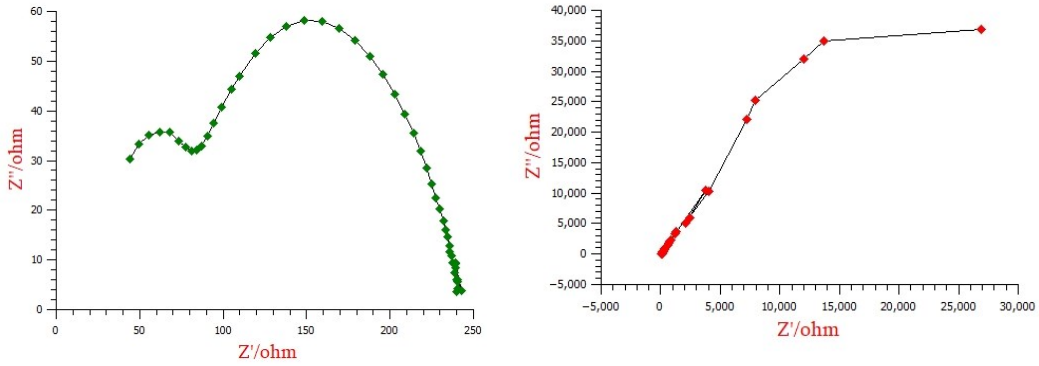

(a) Coated (b) Uncoated

Figure 6 Nyquist Plot for coated and uncoated SS 316L.

An EIS (Electrochemical Impedance Spectroscopy) test was performed at room temperature. The frequency range was swept from 1 Hz to 1 MHz with a 10 mV/min scan rate and 50 logarithmic points. The OCP (Open Circuit Potential) was used as the reference potential. Impedance spectra were taken at the passive potential while the passive film formed. This was ended to examine the stability of the protecting layer on the surfaces of DLC-coated and un-coated SS316L.

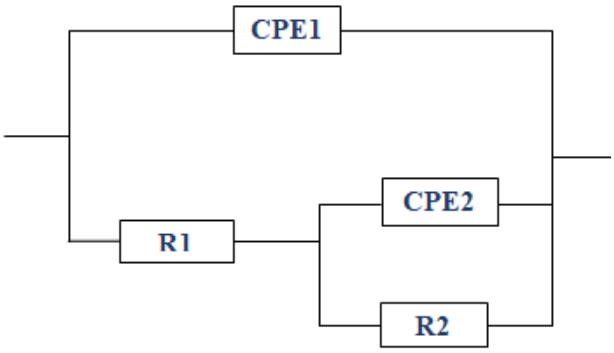

Figure 7 Equivalent electric circuit.

The Equivalent Electric Circuit (EEC) parameters such as Solution Resistance, Charge Transfer Resistance, double layer capacitance, and other relevant parameters can be extracted. These parameters provide valuable information about the electrochemical properties, corrosion behavior, and stability of the protective layers on the studied materials. The comparable electric circuit is depicted in **Figure 7**. A fitting parameter was acquired from EIS test data and was shown to be a good fit for the EEC model. Consequently, the EEC model provided is adequate for determining the behavior of the electrochemical interface through experimentation. The Nyquist plots in **Figure 6** are characteristic of both coated and uncoated SS316L in SBF. The fitting was done using the constant-phase elements, ensuring that the simulated and experimental data agreed.

Potentiodynamic polarization (PDP)

Potentiodynamic polarization curves of coated and uncoated SS316L are shown in **Figure 8**. The corrosion current density (Icorr) decreased with an increase in coating thickness, which indicates that the corrosion product also acts as a barrier to corrosion. The corrosion potential (Ecorr) was more favorable for the DLC-coated SS316L than for the uncoated SS316L, which indicates that the coated SS316L is less likely to corrode [34]. A higher Icorr value (6.587×10^{-6} A/cm^2) indicates a faster corrosion rate, meaning the sample is deteriorating more rapidly. The corrosion current density (Icorr) decreased with an increase in coating thickness, which indicates that the coating thickness also acts as a barrier to corrosion.

The corrosion potential (Ecorr) was measured as the potential difference between the working and reference electrodes. A more noble Ecorr value (−0.256 V) suggests a lower corrosion risk. A more active (less noble) Ecorr value (−0.437 V) indicates a higher likelihood of corrosion. This indicates that the DLC-coated SS316L is less likely to corrode [34].

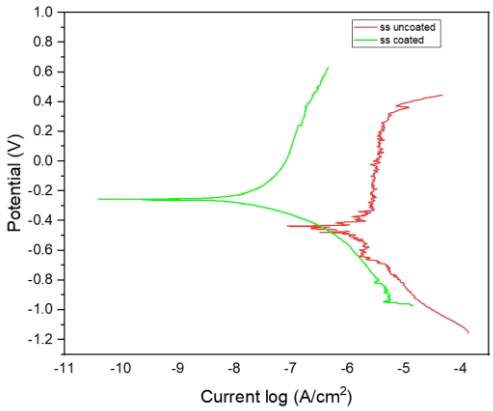

Figure 8 Tafel plot for coated and uncoated SS316L.

The coated SS316L also had a lower breakdown potential, indicating it is more pitting corrosion-resistant [2]. Furthermore [37], in the passive region, the polarization curves of DLC (Diamond-Like Carbon) coated SS316L demonstrate a significant shift in the pitting potential towards more positive

values than the uncoated SS316L. **Table 2** shows the corrosion performance of coated and uncoated SS316L. From **Table 2**, the corrosion potential for DLC-coated SS316L is more noble (positive) than that of the uncoated SS316L in SBF.

Mathematically, the Tafel slope (β) is given by the Stern–Geary Eq. (3);

$$\beta = \frac{2.303\text{xRT}}{\text{nF}} \quad (3)$$

where:
β is the Tafel slope (mV/decade),
R is the gas constant (8.314 J/(mol·K)),
T is the temperature in Kelvin,
n is the number of electrons involved in the electrochemical reaction,
F is Faraday's constant (96,485 C/mol).

According to the tafel plot, the corrosion rate for DLC-coated SS316L is 1.729×10^{-2} mm/year, while the corrosion rate for the uncoated sample is 6.821×10^{-1} mm/year. Mathematically, the Tafel slope (β) is calculated by the Stern–Geary Eq. (3). Materials with lower βa values tend to have better corrosion resistance. The anodic Tafel slope (βa) represents the sensitivity of the corrosion rate to changes in the applied potential [38]. A higher βa value (0.354 V/dec) indicates that the corrosion rate is less sensitive to changes in potential. A lower βa value (0.297 V/dec) suggests that the corrosion rate is more sensitive to potential changes. Similarly, By comparing the cathodic Tafel slope (βc) values of coated and uncoated SS316L, one can assess their relative tendencies for hydrogen evolution [35]. A lower βc value is generally considered to have a lower tendency for hydrogen evolution, making it less prone to hydrogen-related corrosion issues. This indicates that the DLC-coating significantly protects the corrosion rate of SS316L in SBF.

Polarization resistance (Rp) is a crucial electrochemical parameter that quantifies the resistance of a sample to corrosion [38]. Rp is widely used to evaluate the effectiveness of protective coatings in preventing corrosion. A higher Rp value ($2.42\times10^{+6}$ ohm) indicates a lower corrosion rate, suggesting that the DLC is more resistant to corrosion. Conversely, a lower Rp value ($1.516\times10^{+5}$ ohm) implies a higher corrosion rate, indicating a greater susceptibility to corrosion.

Table 2 shows the corrosion performance of coated and un-coated SS316L.

Sample	Icorr value (A/cm^2)	Ecorr value (obs) (V)	βa (V/dec)	βc (V/dec)	Rp (ohm)	Corrosion rate (mm/year)
Uncoated	6.587×10^{-6}	−0.437	0.354	1.624	$1.516\times10^{+5}$	6.821×10^{-1}
Coated	1.669×10^{-7}	−0.256	0.297	0.783	$2.42\times10^{+6}$	1.729×10^{-2}

Surface characterizations

SEM has been used to evaluate the diamond-like carbon-coated and uncoated SS316L surface. It reveals that the surface of the diamond-like carbon-coated SS316L is amorphous and dense over the surface of SS316L, similar to observations found by Jing Wei *et al.* [34], whereas, on the uncoated surface, a lot of delamination and patches are present. For their improved mechanical qualities and biocompatibility, DLC films have attracted more interest as potential biomaterials during the past 20 years [39]. **Figures 9(a) - 9(b)** shows the comparison of coated and uncoated SS316L and (c), (d) before and after the electrochemical test. **Figures 9(c) - 9(d)** Evidence for a DLC protects the surface of SS316L in SBF (pH 7.25) solution at 37 °C. DLC coatings are created by combining poly-type materials in a distinct way to create nanoscale structures that are both formless and adaptive but only have sp3 reinforcement, just like a diamond. This mixture, known as tetrahedral amorphous carbon (ta-C), is the hardest and most grounded.

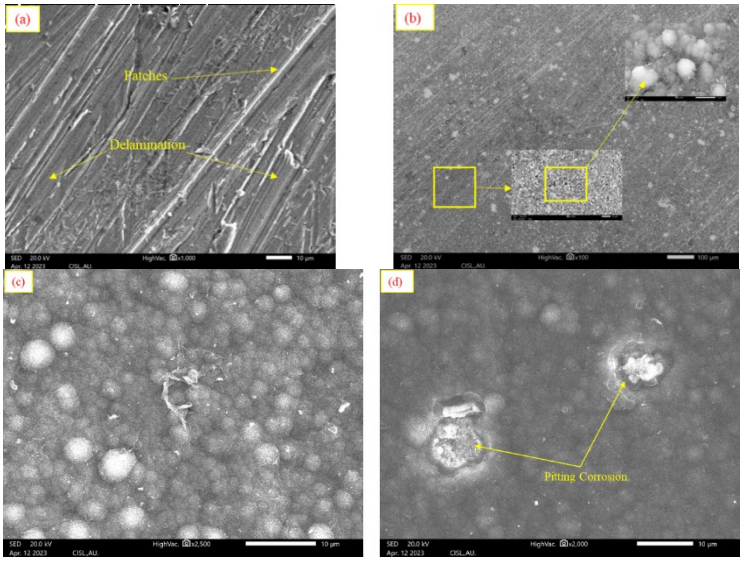

Figure 9 (a), (b) for uncoated and coated SS 316L, and (c), (d) for before and after corrosion test.

The electron dispersive x-ray spectrometer is included here to analyze the elements presented on the coated surfaces SS316L, shown in **Figure 10**. **Figure 10** indicates the highest and lowest percentages of elements presented, i.e., the highest percentage of carbon, 97.26 %, and the lowest percentage of chromium and iron elements presented on the surfaces, 2.58 and 0.17 %, respectively. This suggests that the passive surface layer of the DLC coating is a combination of these elements. A further study used the PVD sputtering technique to deposit soft DLC films with a Cr adhesive interlayer on Si (100), iron, and chrome steel substrates [40]. The C, Fe, and Cr major compositions of DLC coating on steel surfaces were found [33].

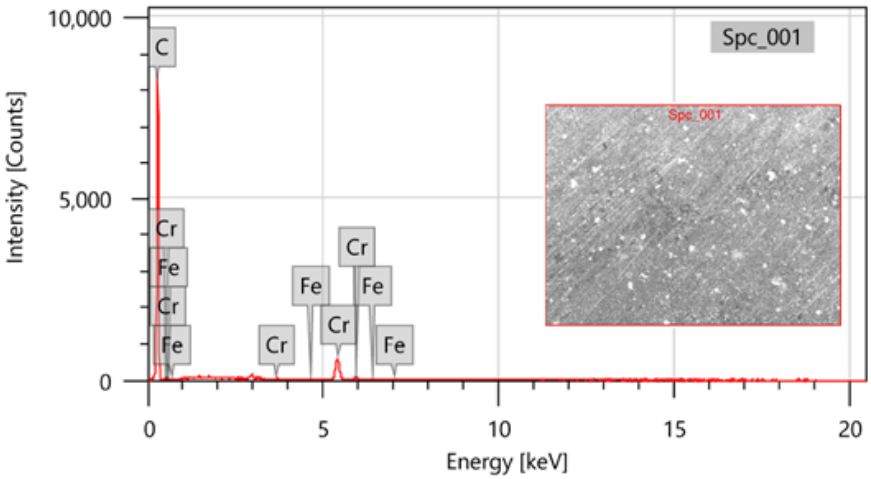

Figure 10 EDS Analysis of the coated SS316L.

Correlation between PDP and EIS

Both techniques provide information about the corrosion mechanism, the corrosion reaction's kinetics, and the corrosion inhibitors' effectiveness. It can be challenging to directly associate the results of these techniques, as each technique provides insights into different electrochemical processes. However, similar conclusions can be drawn by comparing specific parameters from both data sets. In this study, EIS and PP data analysis led to consistent findings. Based on the EIS results, the DLC (Diamond-Like Carbon) coated SS316L exhibited the highest magnitude, with R1+R2 increasing over time. This indicates better corrosion resistance compared to the uncoated samples. Correspondingly, the PDP test revealed that the DLC-coated sample had the highest Rp (polarization resistance) and anodic Tafel slope

(βa), indicating enhanced resistance to corrosion. Additionally, the DLC-coated sample demonstrated a lower current density, further supporting its superior corrosion resistance. By considering the R1+R2 values depicted in **Figure 7** (derived from EIS) and the Tafel and Rp values provided in **Table 2**, the results showed that the DLC-coated SS316L displayed good corrosion resistance along with the uncoated SS316L. It is important to note that although a direct comparison between EIS and PDP results may be challenging due to each technique's different information, a consistent assessment of the DLC-coated sample's superior corrosion resistance was obtained by analyzing relevant parameters from both techniques [41].

Conclusions

Nanoindentation tests examined the mechanical behavior of coated and un-coated SS316L, and the corrosion behavior of coated and un-coated SS316L was examined by electrochemical tests in SBF at 37 °C.

1) Surface morphologies and compositional analysis of the surfaces have been characterized via scanning electron microscopy with EDS, which revealed that the surfaces of the coated SS 316L look smooth and well-structured compared to the un-coated SS 316L, and EDS confirmed that DLC was deposited over stainless steel 316L.

2) The nanoindentation test result indicated that the hardness and elastic modulus of coated SS316L were 15.3 and 162.2 GPa, uncoated samples 354.33 and 33.44 GPa, respectively. It showed that the DLC coating over SS316L improved its mechanical properties compared to uncoated SS316L.

3) According to the Tafel plot, the corrosion rates for DLC-coated SS316L were 1.729×10^{-2} mm/year, while the corrosion rate of the uncoated sample was 6.821×10^{-1} mm/year. This indicates that DLC coating considerably reduces the corrosion rate of SS316L in SBF compared to uncoated SS316L.

4) The EIS result shows that DLC-coated 316L stainless steel has a higher semicircle than un-coated SS316L. This indicates that DLC coating enhances the corrosion resistance of SS316L.

5) The future research interest of the current study is focused on the tribological study of coated and uncoated SS 316L under dry and SBF conditions.

References

[1] S Dwivedi, AR Dixit and AK Das. Wetting behavior of selective laser melted (SLM) bio-medical grade stainless steel 316L. *Mater. Today Proc.* 2022; **56**, 46-50.

[2] N Simionescu, A Ravoiu and L Benea. Electrochemical in vitro properties of 316L stainless steel for orthodontic applications. *Rev. Chem.* 2019; **70**, 1144-8.

[3] C Morsiya. A review on parameters affecting properties of biomaterial SS 316L. *Aust. J. Mech. Eng.* 2022; **20**, 803-13.

[4] P Sivaprakasam, T Hailu and G Elias. Experimental investigation on wear behavior of titanium alloy (Grade 23) by pin on disc tribometer. *Results Mater.* 2023; **19**, 100422.

[5] A Keziz, M Heraiz, F Sahnoune and M Rasheed M. Characterization and mechanisms of the phase's formation evolution in sol-gel derived mullite/cordierite composite. *Ceram. Int.* 2023; **49**, 32989-3003.

[6] A Keziz, M Rasheed, M Heraiz, F Sahnoune and A Latif. Structural, morphological, dielectric properties, impedance spectroscopy and electrical modulus of sintered Al6Si2O13–Mg2Al4Si5O18 composite for electronic applications. *Ceram. Int.* 2023; **49**, 37423-34.

[7] I Alshalal, HMI Al-Zuhairi, AA Abtan, M Rasheed and MK Asmail. Characterization of wear and fatigue behavior of aluminum piston alloy using alumina nanoparticles. *J. Mech. Behav. Mater.* 2023; **32**, 20220280.

[8] S Gharbi, R Dhahri, M Rasheed, E Dhahri, R Barille, M Rguiti, A Tozri and MR Berber. Effect of Bi substitution on nanostructural, morphologic, and electrical behavior of nanocrystalline $La_{1-x}Bi_xNi_{0.5}Ti_{0.5}O_3$ (x = 0 and x = 0.2) for the electrical devices. *Mater. Sci. Eng. B* 2021; **270**, 115191.

[9] M Enneffatia, M Rasheed, B Louatia, K Guidaraa, S Shihab and R Barillé. Investigation of structural, morphology, optical properties and electrical transport conduction of $Li_{0.25}Na_{0.75}CdVO_4$ compound. *J. Phys. Conf. Ser.* 2021; **1795**, 012050.

[10] A Aukštuolis, M Girtan, GA Mousdis, R Mallet, M Socol, M Rasheed and A Stanculescu. Measurement of charge carrier mobility in perovskite nanowire films by photo-CELIV method. *Proc. Rom. Acad. Math. Phys. Tech. Sci. Inform. Sci.* 2017; **18**, 34-41.

[11] P Sivaprakasam, G Elias, PM Prabu and P Balasubramani. Experimental investigations on wear properties of AlTiN coated 316LVM stainless steel. *Mater. Today Proc.* 2020; **33**, 3470-4.

[12] N Sunthornpan, S Watanabe and N Moolsradoo. Elements-added diamond-like carbon film for biomedical applications. *Adv. Mater. Sci. Eng.* 2019; **2019**, 1-11.
[13] L Rui-wu, Z Zhang, L Jian-wei, M Ke-xin, G Yuan-yuan, Z Yan-wen and W Fa-yu. Surface modification of 316L stainless steel by diamond-like carbon films. *J. Iron Steel Res. Int.* 2020; **27**, 867-74.
[14] PA Radi, A Vieira, L Manfroi, KCDF Nass, MAR Ramos, P Leite, GV Martins, JBF Jofre and L Vieira. Tribocorrosion and corrosion behavior of stainless steel coated with DLC films in ethanol with different concentrations of water. *Ceram. Int.* 2019; **45**, 9686-93.
[15] L Natrayan, A Merneedi, D Veeman, S Kaliappan, PS Raju, R Subbiah and SV Kumar. Evaluating the mechanical and tribological properties of DLC nanocoated aluminium 5051 using RF sputtering. *J. Nanomaterials* 2021; **2021**, 8428822.
[16] K Kumari, S Banerjee, TK Chini and NR Ray. Preparation of diamond like carbon thin film on stainless steel and its SEM characterization. *Bull. Mater. Sci.* 2009; **32**, 563-7.
[17] J England, MJ Uddin, E Ramirez-Cedillo, D Karunarathne, S Nasrazadani, TD Golden and HR Siller. Nanoindentation hardness and corrosion studies of additively manufactured 316L stainless steel. *J. Mater. Eng. Perform.* 2022; **31**, 6795-805.
[18] T Kokubo and S Yamaguchi. Simulated body fluid and the novel bioactive materials derived from it. *J. Biomed. Mater. Res.* 2019; **107**, 968-77.
[19] NL Simionescu and L Benea. The corrosion behavior of 316L stainless steel in different simulated body fluids solutions. *Int. Multidisciplinary Sci. GeoConference SGEM* 2017; **17**, 353-60.
[20] M Mehdipour, A Afshar and M Mohebali. Electrophoretic deposition of bioactive glass coating on 316L stainless steel and electrochemical behavior study. *Appl. Surf. Sci.* 2012; **258**, 9832-9.
[21] D Pathote, D Jaiswal, V Singh and CK Behera. Optimization of electrochemical corrosion behavior of 316L stainless steel as an effective biomaterial for orthopedic applications. *Mater. Today Proc.* 2022; **57**, 265-9.
[22] C Tassin, F Laroudie, M Pons and L Lelait. Improvement of the wear resistance of 316L stainless steel by laser surface alloying. *Surf. Coating. Tech.* 1996; **80**, 207-10.
[23] G Li, Q Peng and C Li. Effect of DC plasma nitriding temperature on microstructure and dry-sliding wear properties of 316L stainless steel. *Surf. Coating. Tech.* 2008; **202**, 2749-54.
[24] PA Dearnley and G Aldrich-Smith. Corrosion–wear mechanisms of hard coated austenitic 316L stainless steels. *Wear* 2004; **256**, 491-9.
[25] S Alvi, K Saeidi and F Akhtar. High temperature tribology and wear of selective laser melted (SLM) 316L stainless steel. *Wear* 2020; **448-449**, 203228.
[26] K Zhang, J Zou, T Grosdidier, C Dong and D Yang. Improved pitting corrosion resistance of AISI 316L stainless steel treated by high current pulsed electron beam. *Surf. Coating. Tech.* 2006; **201**, 1393-400.
[27] A Han, JK Tsoi, FP Rodrigues, JG Leprince and WM Palin. Bacterial adhesion mechanisms on dental implant surfaces and the influencing factors. *Int. J. Adhes. Adhesives* 2016; **69**, 58-71.
[28] X Yan, W Cao and H Li. Biomedical alloys and physical surface modifications: A mini-review. *Materials* 2021; **15**, 66.
[29] M Zarka, B Dikici, M Niinomi, KV Ezirmik, M Nakai and H Yilmazer. A systematic study of β-type Ti-based PVD coatings on magnesium for biomedical application. *Vacuum* 2021; **183**, 109850.
[30] A Oktay, H Yilmazer, A Przekora, Y Yilmazer, M Wojcik, B Dikici and CB Ustundag. Corrosion response and biocompatibility of graphene oxide (GO) serotonin (Ser) coatings on Ti6Al7Nb and Ti29Nb13Ta4. 6Zr (TNTZ) alloys fabricated by electrophoretic deposition (EPD). *Mater. Today Comm.* 2023; **34**, 105236.
[31] K Wathanyu, K Tuchinda, S Daopiset and S Sirivisoot. Corrosion resistance and biocompatibility of cold-sprayed titanium on 316L stainless steel. *Surf. Coating. Tech.* 2022; **445**, 128721.
[32] M Jarratt, J Stallard, NM Renevier and DG Teer. An improved diamond-like carbon coating with exceptional wear properties. *Diam. Relat. Mater.* 2003; **12**, 1003-7.
[33] KAHA Mahmud, MA Kalam, HH Masjuki and HM Mobarak. Tribological characteristics of amorphous hydrogenated DLC in the presence of commercial lubricating oil. *Key Eng. Mater.* 2015; **642**, 179-83.
[34] J Wei, P Guo, L Liu, H Li, H Li, S Wang and A Wang. Corrosion resistance of amorphous carbon film in 3.5 wt % NaCl solution for marine application. *Electrochim. Acta* 2020; **346**, 136282.
[35] T Weikert, S Wartzack, MV Baloglu, K Willner, S Gabel, B Merle and S Tremmel. Evaluation of the surface fatigue behavior of amorphous carbon coatings through cyclic nanoindentation. *Surf. Coating. Tech.* 2021; **407**, 126769.

[36] Y Xiao, X Shi, Q Wan and J Luo. Evaluation of failure properties of a DLC/steel system using combined nanoindentation and finite element approach. *Diam. Relat. Mater.* 2019; **93**, 159-67.
[37] M Talha, CK Behera and OP Sinha. Potentiodynamic polarization study of type 316L and 316LVM stainless steels for surgical implants in simulated body fluids. *J. Chem. Pharmaceut. Res.* 2012; **4**, 203-8.
[38] HS Magar, RYA Hassan and A Mulchandani. Electrochemical impedance spectroscopy (EIS): Principles, construction, and biosensing applications. *Sensors* 2021; **21**, 6578.
[39] DK Rajak, A Kumar, A Behera and PL Menezes. Diamond-like carbon (DLC) coatings: Classification, properties, and applications. *Appl. Sci.* 2021; **11**, 4445.
[40] Y Wang, Y Wang, J Kang, G Ma, L Zhu, H Wang, Z Fu, H Huang and W Yue. Tribological properties of ti-doped diamond like C coatings under boundary lubrication with ZDDP. *J. Tribol.* 2021; **143**, 091901.
[41] D Turcio-Ortega, SE Rodil and S Muhl. Corrosion behavior of amorphous carbon deposit in 0.89 % NaCl by electrochemical impedance spectroscopy. *Diam. Relat. Mater.* 2009; **18**, 1360-8.